Published on Marine Geology 281 (2011) 1–13

Possible tsunami signatures from an integrated study in the Augusta Bay offshore (Eastern Sicily–Italy).

Smedile A.[a*], P.M. De Martini[a], D. Pantosti[a], L. Bellucci[b], P. Del Carlo[c], L. Gasperini[b], C. Pirrotta[d], A. Polonia[b], E. Boschi[a]

[a]Istituto Nazionale di Geofisica e Vulcanologia, Sezione Sismologia e Tettonofisica, Via di Vigna Murata 605, 00143 Roma, Italy

[b]CNR - ISMAR - Sede di Bologna - Geologia Marina, Via P. Gobetti, 101, 40129 Bologna, Italy

[c]Istituto Nazionale di Geofisica e Vulcanologia, Sezione di Pisa, Via della Faggiola 32, 56126 Pisa, Italy

[d]Dipartimento di Scienze Geologiche, Università di Catania, Corso Italia 55, 95129 Catania, Italy

*Corresponding author: alessandra.smedile@ingv.it, Istituto Nazionale di Geofisica e Vulcanologia, Sezione Sismologia e Tettonofisica, Via di Vigna Murata 605, 00143 Roma, Italy. Fax: +39 06 51860507, Ph. +39 06 51860572

Abstract

Twelve anomalous layers, marked by a high concentration of displaced epiphytic foraminifera (species growing in vegetated substrates like the *Posidonia oceanica*) and subtle grain-size changes were found in a 6.7 m long, fine sediment core (MS-06), sampled 2 km off the shore of the Augusta Harbor (Eastern Sicily) at a depth of 72 m, recording the past 4500 yrs of deposition. Because

concentrations of epiphytic foraminifera are quite common in infralittoral zones, but not expected at -72 m, we believe that these anomalous layers might be related to the occurrence of tsunamis causing substantial uprooting and seaward displacement of *P. oceanica* blades with their benthic biota.

Our approach involved the study of geophysical data (morphobathymetry, seismic reflection, seafloor reflectivity) and sediment samples, including X-ray imaging, physical properties, isotopic dating, tephrochronology, grain-size and micropaleontology.

Correlations between anomalous layers and tsunami events have been supported by a multivariate analysis on benthic foraminifera assemblage and dates of historical tsunami records. We found that four out of the eleven layers were embedded in age intervals encompassing the dates of major tsunamis that hit eastern Sicily (1908, 1693, 1169) and the broader Eastern Mediterranean (Santorini at about BP 3600). One more layer, even if less distinct than the others, was also defined and may be the evidence for the AD 365 Crete tsunami.

Keywords: Eastern Sicily, offshore core, tsunami, foraminifera.

1. Introduction

Coastal tsunami hazard evaluations include modeling of expected inundations and their frequency in time at a specific site. Therefore, a detailed knowledge of the distribution of past inundated areas and their timing is critical. This information is generally retrieved from historical tsunami catalogues, although these are generally too limited in time and space to be used as the sole reference to forecast the effects and frequency of future events. To overcome this limitation, historical data can be integrated by the geological evidence for inundation from past tsunamis. This approach was tested in several worldwide case studies on low coastal areas, marshes, lagoons, etc. (e.g. among many others Atwater and Moore, 1992; Dawson et al., 1995; Pinegina et al., 2003; Cochran et al., 2006; Scheffers et al., 2008; Shiki et al., 2008) and at a regional scale (Scicchitano et al., 2007, 2010; Pantosti et al., 2008; Barbano et al., 2010; De Martini et al., 2010). Unfortunately, the potential of inland geological studies is substantially reduced by intense coastal urbanization that overprints the natural record. Conversely, offshore studies offer an interesting alternative to the investigation of tsunami's signatures because marine environments can assure a relatively undisturbed continuous record and, therefore, are potentially more sensitive to anomalous events (*i.e*., earthquakes and tsunamis). Although the marine environment might represent a new source for field-based tsunami evidence, very little has been done on the study of tsunami transport and deposition in offshore zones or in shallow-shelf areas (Weiss and Bahlburg, 2006; Dawson and Stewart, 2007). Coarse-grained deposits and, more generally, high-energy processes were used as offshore evidence for past tsunamis (van der Bergh et al., 2003; Reinhardt et al., 2006; Abrantes et al., 2008; Goodman-Tchernov et al., 2009). In addition, these studies highlighted the difficulty of differentiating a tsunami effect from that of normal storms, and faced the problem of a subtle mixing of the two processes in the nearshore zone.

With the aim of exploring new offshore approaches for the paleotsunami research, we started an investigation off the shore of Augusta Bay. We favored this test site for this experiment, because at least 3 large tsunamis (1908, 1693 and 1169) affected this area during the past millennium and there

is onshore evidence for tsunami deposits associated to historical and pre-historical events (Scicchitano et al., 2007, 2010; Barbano et al., 2010; De Martini et al., 2010). Thus, we planned to integrate local on land tsunami deposit studies (De Martini et al., 2010) with offshore coring, to highlight any subtle anomaly in sediments, fauna assemblages, physical properties, etc., that could represent a proxy for tsunami occurrence.

Differently from previous offshore studies in this area (Di Leonardo et al., 2007; Budillon et al., 2005; 2008) that considered only the recent part of sediments (i.e. the first 30 cm bsf), this paper presents new data from a 6.7 m-long core sampled in the northern part of the bay, in shelf mud deposits where no evidence of gravitational processes and anthropogenic disturbances (both in terms of sediment quality and of local sedimentation rate due to dumping) exist.

2. The Augusta Bay

Augusta Bay in SE Sicily is a wide gulf facing the Ionian Sea, showing a rather smooth morphobathymetry, with maximum depths reaching 100-120 m at the shelf-break (Fig. 1A). The bay area, hosting Sicily's major harbor and several large petrochemical industries, has been recognized as a high environmental risk site, both by the World Health Organization (Martuzzi et al., 2002) and the Italian Government (G.U.R.I., L. 426/1998). Recently published offshore works in Augusta Bay are mostly focused on the effects of industrial activity and related contaminants (especially Hg) in the marine environment, as well as their impact on the present benthic foraminifera communities and the coastal ecosystems as a whole (Decembrini et al., 2004; Raffa and Hopkins, 2004; Di Leonardo et al., 2007; 2009). Detailed ^{210}Pb profiles estimate an average sediment accumulation rate that varies from 1.6 to 5.3 mm y^{-1} moving offshore (Di Leonardo et al., 2007). Moreover, Budillon et al. (2005) revealed possible sediment dumping sites at several places on the shelf, probably due to the continuous standard dredging operation in the inner harbor. Thus, the artificial modification of offshore sediment interface might have locally resulted in an unusually high sedimentation rate. In an integrated study on box-corer samples, Budillon et al. (2008)

observed that a discontinuous muddy layer, enriched in shells, and rodholites mixed with reworked *Posidonia oceanica* remnants, occurs in the mid-shelf at a depth of 10-30 cm below the sea floor. This peculiar layer was interpreted as the pre-industrial seabed, covered and sealed by a mud drape characterized by higher concentrations of pollutants and the lack of living macro fauna.

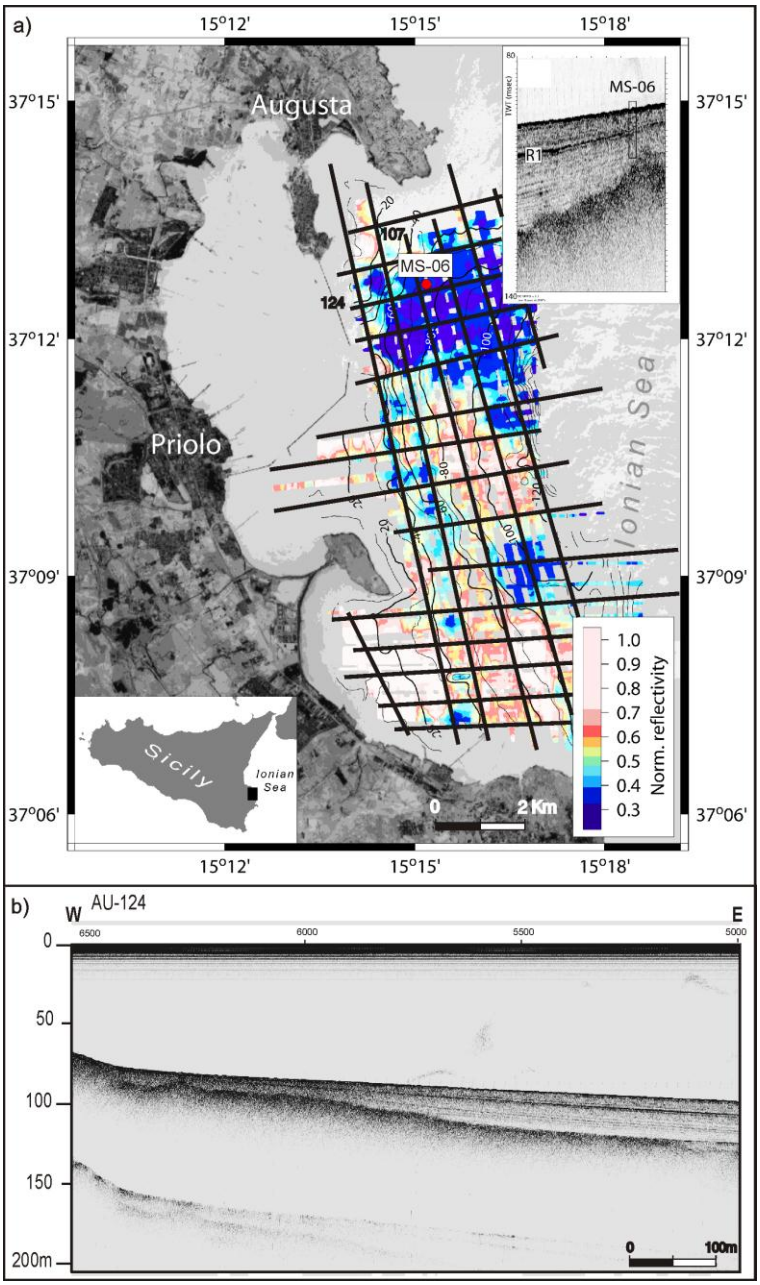

Fig. 1. A) Map of the investigated area compiled using: aerial photo; bathymetric contours (spacing 5 m), color-scaled reflectivity of the seafloor (blue (dark gray in B/W version)=low reflectivity; red (light gray in B/W version)=high reflectivity). Location of the core MS-06 (red dot) and chirp-sonar seismic lines (black lines) are indicated. B) AU-124 chirp profile, note the presence of a transparent sedimentary sequence with the coarser layers and of the continuous highly reflective layer (see location in A).

2.1 Site selection by geophysical survey

Taking into account the above mentioned studies, we chose the sampling area on the basis of the analysis of a close-spaced grid of seismic reflection chirp-sonar profiles covering the 150 km^2 of the bay. These profiles image the Holocene sedimentary sequence, up to a strong erosive unconformity that marks the LGM (Last Glacial Maximum), and enabled us to compile a bathymetric/seafloor-reflectivity map (Fig. 1A). The bay appears characterized by a narrow shelf and a relatively steep slope (slope value from 2% to 4%) located approximately 5 km from the shoreline. Seismic lines highlight the presence of an uppermost nearly transparent, homogeneous sedimentary sequence unconformably laying over the acoustic bedrock (Fig. 1B) likely made of Miocene to Pleistocene terrains, which outcrop extensively onshore. The thickness of the Holocene sequence appears highly variable in the area, with extensive bedrock exposures, particularly frequent in the S sector. The imaged sequence is characterized by the presence, within the Holocene deposits, of one prominent reflector that can be correlated over the entire Augusta Bay area. Other less prominent reflectors are also visible (Fig. 1B). The high-reflectivity layers likely mark the presence of coarser deposits, within a mud-dominated sedimentary sequence.

The close-spaced grid of chirp-sonar profiles also enabled us to obtain a rough seafloor characterization. Although propagation and scattering of high frequency acoustic sound at or near the bottom is controlled by a number of factors, the most important geotechnical property related to acoustic attenuation is the average grain-size of the insonified sediment (e.g., Shumway, 1960; Dunlop, 1992; Gasperini, 2005). Calculating the seafloor reflectivity at each ping, along each profile, we obtained a reflectivity map of the seafloor where areas characterized by low reflectivity coincide to the presence of fine sediments. By combining reflectivity and morphobatymetric data (Fig. 1), we observed that the northern part of the bay is characterized by a wider shelf and fine-grained lithologies (low-reflectivity, blue colors in Fig. 1A, dark gray in the B/W version); to the S, more complex morphologies and high-reflectivity patterns prevail.

Where the acoustic signal penetrates the sub-seafloor, we observed an undisturbed sedimentary sequence (Fig. 1B) without major geometrical unconformities, and the absence of features possibly related to erosive/re-depositional processes caused by the effects of currents or gravitational failures.

Given all of the above, the northern part of the bay was selected as the ideal location to sample a complete Holocene stratigraphic record. In fact, a 6.7 m-long sediment gravity core (MS-06) was collected from the CNR R/V *Urania* in 2007, about 2 km off the coastline, at a depth of 72 m (Fig. 1A).

3. Methodology and results

3.1 X-ray imaging and physical properties

The MS-06 core was studied through several approaches that firstly included a visual description, X-ray imaging and high-resolution laboratory measurements of physical properties (low field magnetic susceptibility and bulk density at the GEOTEK Multi-Sensor Core Logger (MSCL-S) facility of the IAMC-CNR Petrophysical Laboratory of Naples).

The MS-06 core is made of 6.7 m of almost homogeneous mud, interrupted by a 3-4 cm thick black medium-coarse sandy layer at ~3 m below the top (Fig. 2). A quite thick *Posidonia oceanica* rich layer appears as a discrete interval just below the top core also highlighted as a darker horizon by X-Ray imaging (Fig. 2A). Further dark layers, likely related to the compaction of *P. oceanica* remains, are recognizable in a qualitative way along the core from X-ray imaging, as well as localized concentrations of molluscs (mainly *Turritella communis*), sometimes arranged without directional pattern (Fig. 2B).

The gamma density profile shows a homogeneous pattern with minor fluctuations, confirming that the core was sited in a low energy environment with a monotonous deposition dominated by fine-grained sediments (Fig. 2). The magnetic susceptibility profile highlights the presence of a single layer very rich in magnetic minerals coinciding with the black medium-coarse sandy layer

highlighting its volcanic origin (Fig. 2).

Additionally, inorganic element composition using an ITRAX X-ray fluorescence (XRF) core scanning for non-destructive analysis was carried out at the Eastern Mediterranean Centre for Oceanography and Limnology (EMCOL) in Istanbul. Unfortunately, XRF results did not provide any significant trend in the elements nor correlation between any of them and the other characteristics of the cored sediments, most probably because of the long time elapsed (almost 2 yrs) between the coring and the analysis that resulted in a significant drying process of the sediments.

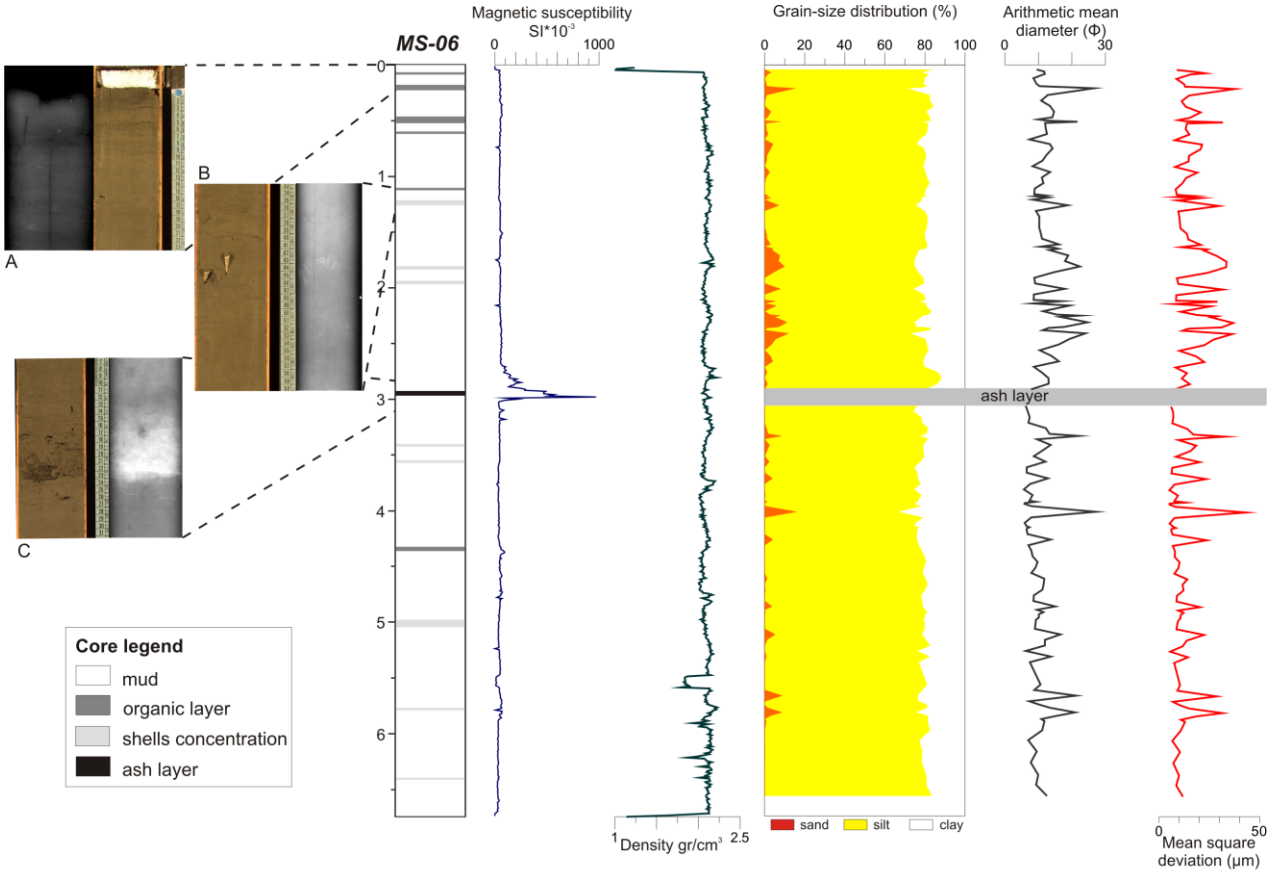

Fig. 2. Simplified lithology of core MS-06 compared to magnetic susceptibility, γ density logs and grain-size distribution with some derived parameters. On the left side some details of sediments and X-ray images: A) uppermost portion with organic layer rich in Posidonia fibers, B) shells concentration layer and relative X-ray image, C) ash layer consisting of black fine lapilli and coarse ash.

3.2 Grain-size analysis

For grain-size determination, core sediments were sampled each 5 or 2 cm depending on the proximity to intervals that appeared to contain changes from the visual inspection. The material was soaked in H_2O_2 and dispersed with sodium hexametaphosphate (1%). Afterwards, the samples were analyzed with a Fritsch-Analysette 22 laser particle counter at the EMCOL laboratory in Istanbul. To prevent any damage to the instrument (characterized by a measuring range of 0.3-300 μm), we did not sample the 15 cm core section centered on the volcanic sandy layer.

The sedimentological analysis was performed on 154 samples and confirmed that the core is dominated by fine-grained sediments with prevailing silt content (average 79%), with the black volcanic medium-coarse sandy layer being the only exception (Fig. 2). The second class in order of abundance is clay with an average of 19%, followed by fine to very fine sand (2% as average). Nearly half of the analyzed samples show a null value for the latter grain-size, thus suggesting that the fine to very fine sand is exceptionally uncommon at the MS-06 site, and occurring only in specific portions of the core. Moreover the no-null value sand samples tend to be grouped in somehow distinctive layers. Significant sand percentages up to 16%, well above the average value of 2%, characterize some of these layers (Fig. 2).

3.3 Foraminiferal analysis

Sixty-eight 1 cm-thick samples were collected with different spacing (from 1 to 25 cm) for foraminiferal analysis. Samples were: (i) soaked in water added with hydrogen peroxide (5%); (ii) wet sieved through sieves of 63 μm (230 mesh) and 125 μm (120 mesh); (iii) dried again.

All the cleaned samples show high amounts of fibers from the seagrass *Posidonia oceanica* and few small molluscs (e.g. *Turritella communis, Nucula sulcata* and *Venus* sp.).

In this study data from >125 μm size fractions were employed, while the 63-125 μm fraction was preserved for future researches. In order to diminish the effects of sorting according to size and shape of the specimens over the tray to split the sediment, the following procedure was adopted: (1)

part of the sediment was firstly thrown in a corner; (2) the left fraction was distributed as evenly as possible over the rectangular gridded picking tray. This procedure permitted us to leave the larger forms in the first throwing. At least 300 benthic foraminifera specimens were separated and identified and relative percentages were calculated for each species. Planktonic foraminifera, due to their low number in each sample, were simultaneously counted and identified at a generic level. For each sample the [P/(P + B)]% ratio (where P represents the number of planktonic foraminifera in the sample and B the number of benthic foraminifera in the same sample) was also calculated, because it is normally assumed to be correlated to bathymetry increasing (Van der Zwaan et al., 1990, and references therein). The identification of benthic species was supported by original descriptions and several key papers like AGIP (1982), Cimerman and Langer (1991), Sgarrella and Moncharmont Zei (1993), Fiorini and Vaiani (2001).

Approximately 222 benthic foraminifera species belonging to 89 genera have been identified. The 19 most abundant benthic taxa (those >5% in at least one sample) were used to create the final matrix (supplementary material Table 1 and 2) that was processed through a multivariate analysis (Q-mode and R-mode Hierarchical Cluster Analysis), using statistical software (PAST-Paleontological Statistic-ver. 1.93 by Hammer et al., 2001 and described by Hammer and Harper, 2006). The Hierarchical Cluster Analysis (HCA) segregates entities (samples, species, measurements) into "naturally occurring" groups and quantifies the between-group relationships (Parker and Arnold, 1999). Analyses are referred to as Q-mode for clustering samples, or R-mode for clustering of environmental variables (e.g. species).

R-mode cluster analysis on foraminifera fauna provides information about their community structure, revealing two main clusters, A and B, which we used to define the relative assemblages (Fig. 3A). The dendrogram of sample associations obtained performing Q-mode analysis is substantially in line with these associations. In fact, Q-mode analysis highlights the presence of three distinct clusters (Fig 3B): Qa and Qc correlate with Cluster A, and Qb correlates to Cluster B. Figure 4 shows how the Qb samples can be grouped forming layers often centered on a peak value.

In the following paragraphs we describe the assemblage content, their palaeo-environmental meaning and their distribution in the study core.

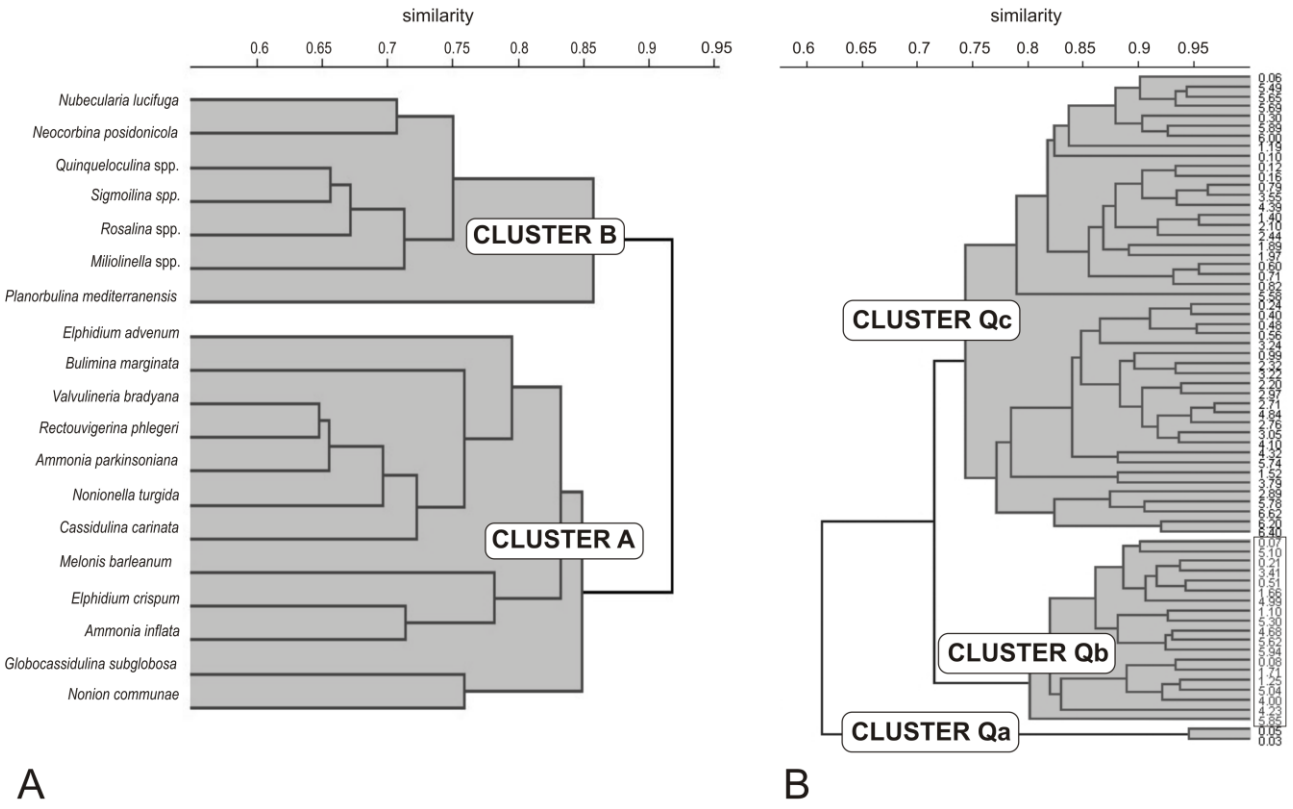

Fig. 3. Dendrogram classifications resulting from multivariate cluster analysis based on the relative abundance of the 19 most common benthic foraminifera taxa. A) Foraminiferal assemblage produced by R-mode analysis using Horn's (1966) modified version of Morisita's (1959) index; B) Sample associations produced by the Q-mode analysis performed with a Morisita's distance. Cluster B is well correlative of Cluster Qb and concur in the definition of 11 anomalies in the core.

1. Cluster A consists of several taxa showing a considerable variety of species and a fluctuating trend. Foraminifera species from this cluster display the highest relative abundance recorded throughout the core sequence (up to the 70% of the benthic assemblage). The two main species are *Ammonia inflata* up to 18% and *Nonionella turgida* up to 23% while other species as *Ammonia parkinsoniana, Bulimina marginata, Elphidium crispum, E. advenum, Globocassidulina subglobosa, Melonis barleanum, Nonion communae, Rectouvigerina phlegeri, Valvulineria bradyana* show abundances of up to 10%. Samples including this species association are grouped in

Cluster Qc and Cluster Qa (where Qa contains the topmost samples in which *Nonionella turgida* has the highest values).

Variety and composition of this assemblage is consistent with an intermediate depth (inner-shelf) and a muddy substratum rich in organic matter (biofacies IV of Jorissen, 1987), as testified by high values of *Nonionella turgida*, considered an opportunistic species that prefers high food availability and tolerant to reduced oxygen conditions (Van der Zwaan and Jorissen, 1991).

2. Cluster B consists of several taxa (Fig. 3A) dominated by *Nubecularia lucifuga* and *Neocorbina posidonicola* and secondary taxa *Planorbulina mediterranensis, Sigmoilina* spp. *(S. costata* and *S. grata), Miliolinella, Quinqueloculina* and *Rosalina* groups. As for the association of the previous cluster, the species belonging to Cluster B show a fluctuating trend and several peaks up to 57% of the total assemblage. This association is consistent with those samples included in Cluster Qb (samples encircled in Fig. 3B) where based on a quick inspection these taxa are present with a percentage >25% (Fig. 4). All the taxa in this cluster are epiphytic specimens (species living on seaweed and seagrass) and according to their way of life have also been divided informally into four morphotypes by Langer (1993). Since this latter subdivision, in Cluster B we recognize three of the four morphotypes: (A) stationary, permanently attached forms that occur mainly on the broad leaves of *Posidonia oceanica* and *Sargrassum hornschuchi* (it forms 5-62% of the assemblage at depths of 15-30 m); (B) temporarily attached forms with a flat attachment surface; and (D) permanently motile, grazing epiphytes. The absence of the morphotype C (suspension feeding motile species) in this cluster can be explained by the fact that species belonging to this morphotype (mainly elphidids) may not share similar behavioural strategies or microhabitats (Langer, 1993).

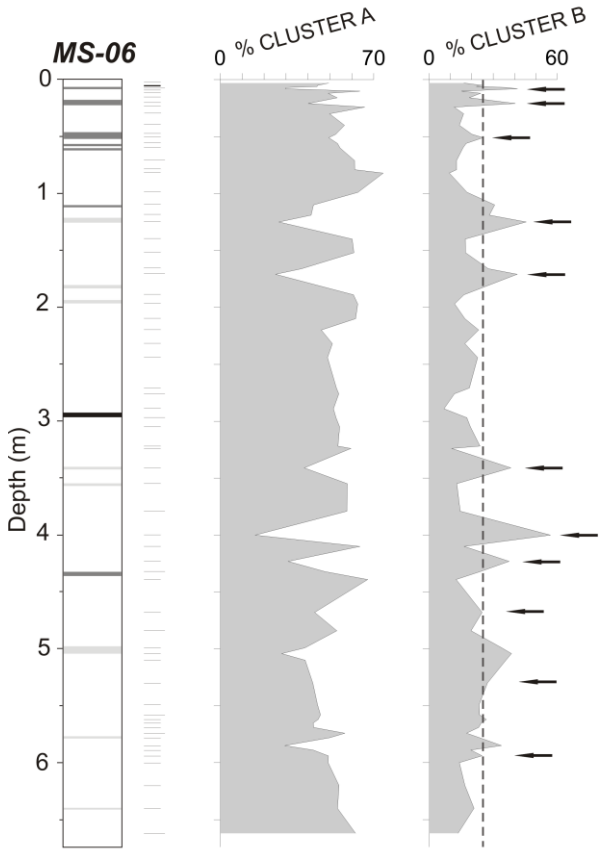

Fig. 4. Downcore distribution of the cumulative percentages of the two Clusters A and B and the P/B ratio. The vertical dashed line in Clusters B fix up the threshold of 25% highlighting those samples from the Cluster Qb in which the considered species (epiphytic taxa) show higher percentages. Samples from Cluster Qb can be grouped forming layers, often centered on a peak value, and the black arrows indicate the deeper sample of each samples group. For legend of the core log see also Fig. 2.

Cluster B epiphytic foraminifera normally live in the infralittoral zone (lower limit 45-50 m *sensu* Perés and Picard, 1964) on vegetated and coarse substrates, such as the *P. oceanica* (following the morphotype classification especially on broad leaves). In detail, *P. oceanica* is a marine phanerogam seagrass endemic to the Mediterranean basin and widespread along its coast in a bathymetric range from the surface to 30-40 m bsl in clear waters (Pergent et al., 1995). Because of their way of life, epiphytic foraminifera together with *P. oceanica* remains can be also dispersed deeper by bottom currents and, for this latter reason, can be considered as displaced in the core. Nevertheless, as highlighted by samples included in Cluster Qb, in at least 11 cases (Fig. 4), epiphytic specimens are observed in very high concentrations (from 25% to 57% of the total assemblage). These 11 displacement cases should have been related to an exceptional cause that

brought high dispersion of these species at greater depths (72 m bsl) relative to their life zone (up to 35-40 m bsl considering the depth limit of the *P. oceanica*).

Differently from the benthic assemblage, planktonic foraminifera are present in limited amounts and their assemblage principally consists of *Globigerina* spp. and *Globigerinoides* spp (see supplementary material Table 1). As previously seen for the R-mode clusters analysis, the P/B ratio shows a fluctuating trend too (Fig. 4). This distribution seems to reflect the presence of the displaced epiphytic specimens that likely drowned the living assemblage. In fact, in most of the 11 displacement cases the P/B ratio shows a decreasing trend. Nevertheless, the P/B ratio, that ranges from 1.61% to 14.24%, seems to be consistent with a core collected at a water depth of 72 m indicating that no significant bathymetric changes took place (Fig. 4).

3.4 Composite chronologies

We used a series of dating methods to better chronologically constrain the MS-06 core: radiocarbon dating, radioactive tracers (^{210}Pb and ^{137}Cs) and tephrochronology.

Ten samples (marine mollusks and foraminifera shells) were ^{14}C dated at the AMS facility of the Poznan Radiocarbon Laboratory (Table 1); measured ages were dendrochronologically corrected according to the radiocarbon calibration program OxCal 4.1 (Bronk Ramsey, 2009), using a marine calibration curve that incorporate a time-dependent global ocean reservoir correction of about 400 years (Reimer et al., 2009). Moreover, the marine palaeo-reservoir effect was subjected to the local effect (ΔR offset) that, in the Mediterranean Sea, appears to be relatively constant for the past 6 or 7 ka (Reimer and McCormac, 2002). The appropriate ΔR offset can be selected from the Chrono Marine reservoir Database (Reimer and Reimer, 2001). Because of the lack of a local ΔR value, and considering that shelf waters along the eastern Sicilian coast are influenced by an enriched water mass (Messina Mixed Water) formed in the Messina Strait and transported southward (Raffa and Hopkins, 2004), we decided to adopt an average value of 124±60 yr derived from the two nearest sites (Tyrrhenian coast of Sicily, IT and Zante, GR).

These calibrated ages appear to be coherent and in stratigraphical order, with a unique exception for the sample prepared with mixed foraminifera that resulted older than samples collected up to 1.5 m below, and consequently discarded in the present study (Table 1). Considering the 2σ distribution of the dated samples the base of the MS-06 core has a maximum radiocarbon calibrated age of ca. 4500 yrs. The derived sedimentation rates calculated between dated samples seems to be quite constant with an average value ranging from 1.5 to 2 mm/yr along the core. An exception is represented by the uppermost part of the core where the sedimentation rate decreases to 0.7 mm/yr.

Table 1

Results from ^{14}C-AMS dating and samples calibration from core MS-06

Sample code	Lab code	depth (m)	Sample type	$\delta^{13}C$	Measured Age BP	Cal curve	1 or 2 σ	Cal AD/BC ranges	
								min.	max
MS-06 48-49	Poz-24606	0.48	marine shell	0,8	1495±30	Marine 09	1	AD 960	AD 1125
			(*Turritella*)				2	AD 885	AD 1200
MS-06 82-84	Poz-22913	0.84	marine shell	-0,1	1655±35	Marine 09	1	AD 785	AD 950
			(*Venus*)				2	AD 715	AD 1015
MS-06 125-127	Poz-22914	1.27	marine shell	6,8	1820±30	Marine 09	1	AD 640	AD 775
			(*Nucula*)				2	AD 570	AD 855
MS-06 179	Poz-24607	1.79	marine mollusk	-1,2	1960±30	Marine 09	1	AD 495	AD 650
			(*Turritella*)				2	AD 420	AD 690
MS-06 276-278	Poz-20877	2.78	marine shell	-1,7	2330±30	Marine 09	1	AD 70	AD 235
			(*Venus*)				2	BC 20	AD 325
MS-06 305-306	*Poz-20876*	*3.06*	Mixed	*2,1*	3305±35	Marine 09	1	BC 1125	BC 920
			Foraminifera				2	BC 1240	BC 845
MS-06 355-357	Poz-22915	3.57	marine shell	-1,6	2680±35	Marine 09	1	BC 360	BC 195
			(*Nucula*)				2	BC 435	BC 80
MS-06 467	Poz-22916	4.67	marine shell	5,5	2925±35	Marine 09	1	BC 720	BC 505
			(*Nucula*)				2	BC 755	BC 400
MS-06 562-563	Poz-22917	5.63	marine shell	6,4	3270±35	Marine 09	1	BC 1085	BC 890
			(*Nucula*)				2	BC 1185	BC 810
MS-06 -1	Poz-20875	6.63	marine shell	3,4	4245±35	Marine 09	1	BC 2340	BC 2125
			(*Turritella*)				2	BC 2440	BC 2030

Ages were dendrochronologically corrected according to the radiocarbon calibration programs OxCal 4.1 (Bronk Ramsey, 2009) using a marine calibration curve (Reimer et al., 2009) with an appropriate ΔR offset (124±60) selected from the Chrono Marine reservoir Database (Reimer and Reimer 2001). The dating in *italic* corresponds to a sample not considered for the age model.

The short-lived radionuclides ^{210}Pb and ^{137}Cs were analysed on the uppermost 40 cm of the core; ^{210}Pb was analysed via alpha spectrometry of its granddaughter ^{210}Po, assuming secular equilibrium. The excess ^{210}Pb ($^{210}Pb_{ex}$) was calculated by subtracting the supported fraction from the total. ^{137}Cs activities were determined directly via gamma spectrometry on dry sediments. Details of the methods can be found in Bellucci et al. (2007). The $^{210}Pb_{ex}$ profile was used to calculate a mean sedimentation rate, assuming constant flux of the radiotracer and constant sedimentation (Robbins, 1978; Appleby and Oldfield, 1992); the relatively low value of ^{210}Pb in the topmost samples suggests a moderate (few cm) loss of sediment from the top of the core, due to the sampling method. The presence of ^{137}Cs only in the superficial levels (0-3 cm) confirms the ^{210}Pb derived chronology (Fig. 5A) that yields an average sedimentation rate for the uppermost 15 cm of 0.7 mm/yr.

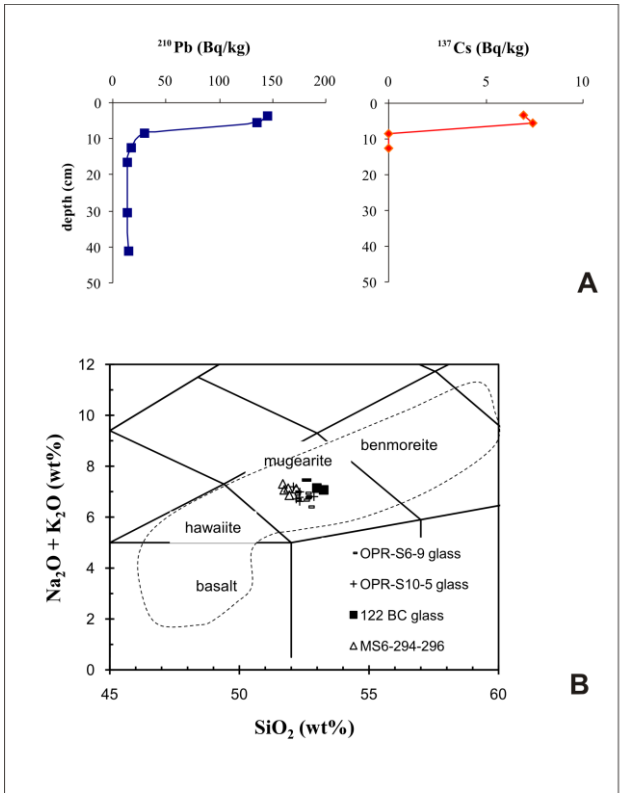

Fig. 5. A) Results from the ^{210}Pb and ^{137}Cs activity-depth profiles in the top section of MS-06 core. B) Total Alkali Silica classification diagram (TAS; Le Bas et al., 1986) showing glass compositions of the BC 122 tephra recovered in MS6 core (this study), Priolo Reserve site (OPR-S6 and OPR-S10 cores) and on Etna flanks for comparison (modified after De Martini et al., 2010). Dashed line includes the composition of Etna volcanics (Corsaro and Pompilio, 2004).

To investigate the possible attribution of the 3 cm-thick black medium-coarse sandy layer (tephra layer recovered at 2.96 m in Fig. 2) to a known and dated eruption, an optical microscope was used to analyze its particles for a petrographic and morphoscopic analyses; whereas, the glass composition was analysed in the sideromelane clasts using a LEO-1430 scanning electron microscope, equipped with an Oxford EDS micro-analytical system (SEM-EDS) at INGV Sezione di Catania laboratories (Supplementary material Table 3). Analytical conditions were 20 keV of acceleration tension, 1200 nA of beam current and XPP data reduction routine. To minimize alkali loss during analysis, a square raster of 10 micron was used. Replicate analyses of the international standard VG-2 glass basaltic (Jarosewich et al., 1980) were performed for analytical control. The precision expressed as relative standard deviation was better than 1% for SiO_2, Al_2O_3, FeOtot and CaO and better than 3% for TiO_2, MnO, Na_2O, K_2O and P_2O_5. The tephra deposit is composed of well vesicular scoriaceous clasts (sideromelane and tachylite), loose crystals of plagioclase, minor olivine, clinopyroxene and lava lithics. Glass composition of sideromelane clasts in the total alkali versus silica diagram (TAS; Le Bas et al., 1986) shows alkaline affinity as Etna volcanics and mugearitic composition (Fig. 5B). Petro-chemical and morphoscopic analyses of MS-06 tephra are analogous to the tephra fallout deposit produced by the BC 122 plinian eruption of Etna (Coltelli et al., 1998, Del Carlo et al., 2004), recovered in the Priolo Reserve cores (onshore of Augusta Bay – De Martini et al., 2010) and on Etna flanks (Fig. 5B).

Given all the aforementioned data that provide compatible chronological constraints for the MS-06 core, we attempted the construction of a depositional model (Fig. 6). For this purpose we used a P_Sequence (Bronk Ramsey, 2008), a Bayesian model of deposition implemented by the computer software OxCal 4.1 (Bronk Ramsey, 2009). Given that the marine sedimentation cannot be regarded as perfectly constant, the P_Sequence depositional model takes into account the uncertainties of the sedimentation rate variations, by considering sedimentation as an inherently random process. The

resulting age model reflects the increasing uncertainties with distance from the calibrated sample ages (Fig. 6).

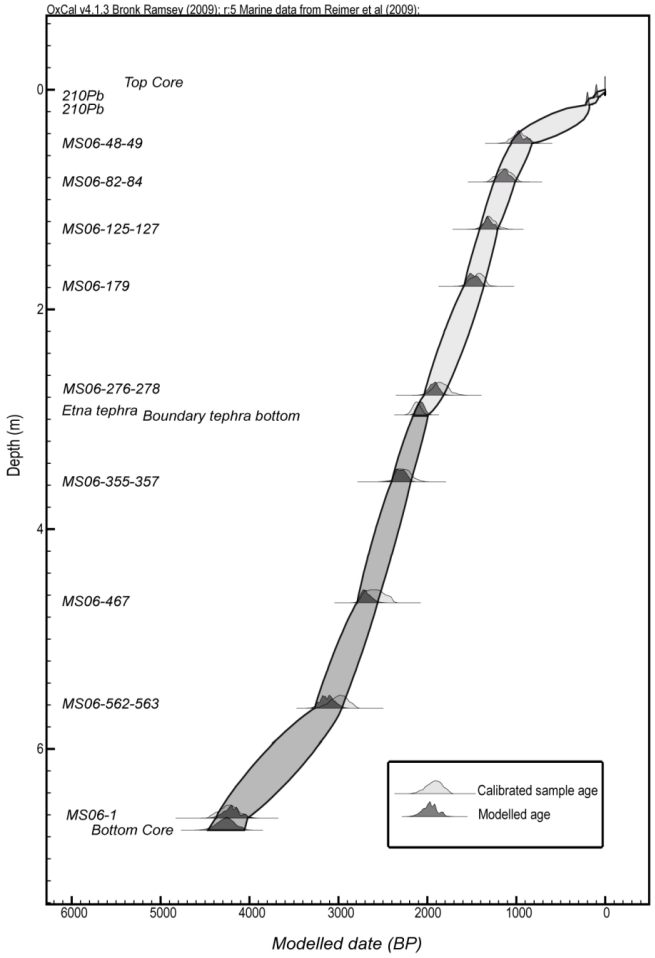

Fig. 6. Age depth model output for the MS-06 core using depth as the variable and assuming the deposition is a Poisson process (P_sequence from OxCal 4.1 software, Bronk Ramsey, 2009) with a value of 20 for both the parameters k and s (increments per unit length and number of automatically generated depth model points per unit length, respectively).

As a consequence, the uncalibrated age of the bottom core boundary is estimated with a wide margin, being only constrained by the deepest sample age, while the top core age is confined by the calibrated age of the seafloor at the time of sampling. Finally, the regularity of the sedimentation process is determined by factor k, with the higher values of k reflecting smaller variations in sedimentation rate (Bronk Ramsey, 2008). We chose the highest possible values of k, so that the modeled age fit each individual calibrated age. We used k =20 for the MS-06 core obtaining the 68% and 95% probability ranges plotted in the calibrated age vs. depth model (Fig. 6).

In the P_Sequence model we input: (1) uncalibrated ^{14}C ages and their relative sample depths (main dataset); (2) ^{210}Pb derived ages (as calibrated ages); (3) Etna tephra age (expressed as calendar age to be integrated with ^{14}C ages) and relative depth; (4) a boundary limit at the base of the tephra, because it likely represents a relevant change in the sedimentation.

The P_Sequence model confirms an age of ca. 4500 yrs for the base of the core and suggests an average sedimentation rate of 1.7-2.1 mm/yr for the entire core (calculated from 0.49 m to 6.74 m), apart from the uppermost part (from the top to 0.49 m) showing 0.4-0.6 mm/yr (similar to the 0.7 mm/yr rate suggested by short-lived radionuclides). Differently from previous studies (Di Leonardo et al., 2007; Budillon et al., 2008), this P_Sequence model does not highlight important anthropogenic disturbances in the youngest part of the MS-06 sequence (past 50-60 yr).

4. Combined evidence for high-energy events and estimate of their timing

Seismostratigraphic analysis of the close-spaced grid of high-resolution chirp profiles was used to avoid possible damping areas related to the petrochemical and harbor activities and in the selection of a proper coring site. Furthermore, chirp profiles enabled us to detect only one major unconformity in the Holocene sequence that it is related to the BC 122 tephra layer. Chirp profiles highlight other small high reflectivity layers, indicating a possible change in the grain-size (Fig. 1) but we could not relate them to any specific layer. A more detailed work on the geophysical data is in progress to explore potential anomalies and correlations with the MS-06 core. For this reason, we explored the possibility of more subtle evidence in the sedimentary record through different laboratory techniques.

Results from benthic foraminiferal assemblage analysis have shown up to 11 intervals (samples forming the Cluster Qb and B) in which displaced epiphytic foraminifera are present with abundance >25% of this whole assemblage (Fig. 4). An opposite trend was found in the P/B ratio that shows a negative deflection in correspondence of almost all benthic displacement cases. This is tentatively explicable with a likely drowning of the total living assemblage caused by the external

heavy inputs of displaced epiphytic specimens from the nearshore (Fig. 4). Moreover, the sedimentological analysis highlights sandy inputs in these 11 anomalous intervals (Fig. 7). Because the coincidence between levels showing sandy input and those characterized by peculiar epiphytic foraminifera abundance is not univocal, we analyzed in detail all the layers enriched in coarser grains. In doing this, we selected a total number of 19 distinct levels. We noted that the average abundance of sand for the 11 intervals matching with Cluster Qb samples is almost double (8.1%) with respect to the unmatched ones (8 samples with 4.6%). Moreover, an inspection of the grain-size distribution of the two most prominent layers with sandy input (collected at 0.21 and 4.00 m depth), matching with Cluster Qb samples, show that they contain a more pronounced enrichment of the sandy part (see grain-size bimodal distribution graphs in Fig. 7), with respect to those intervals (collected at 0.96 and 4.86 m depth) characterized by a sandy input but uncorrelated to Clusters B/Qb or to those collected above and below them (at 0.19, 0.32, 0.91, 1.01, 3.96, 4.06, 4.81 and 4.89 m depth, Fig. 7). A similar bimodal distribution has been observed in most of the sandy input intervals matching with Cluster Qb samples but it is not so clearly outstanding with respect to 0.21 and 4.00 m depth samples shown in Fig. 7. This bimodal distribution may be interpreted as the result of different depositional mechanisms and/or different sources for the sand.

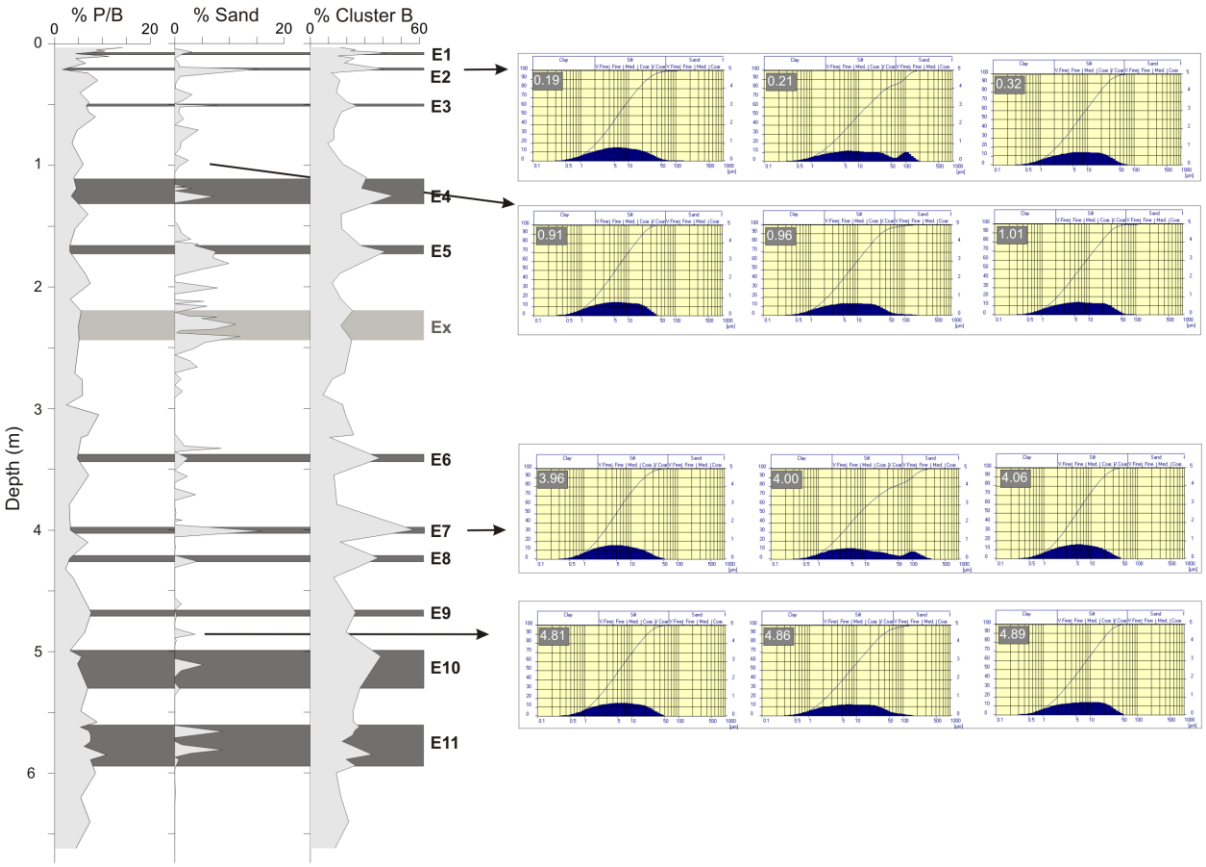

Fig. 7. Correlation between P/B ratio, sand distribution and the layers (highlighted by samples in Cluster Qb) in which epiphytic species (Cluster B) are present with percentage >25%. The layers are numbered from the top to the bottom. In light gray the additional layer Ex.
On the right side, grain-size distribution plots of the two most prominent sandy intervals matching with Cluster Qb samples and two samples characterized by a sandy input but uncorrelated to Clusters Qb. Of the plots triplets the central one is the sample with the sandy inputs, while the others are the samples collected just above and below it (numbers on the left upper corner represents the samples depth).

It is noteworthy that the topmost interval at 0.08 m depth also corresponds to a few mm-thick *P. oceanica* fiber rich layer that appears as a discrete layer by macroscopic observation and X-ray imaging (Fig. 2A). Moreover, some other Cluster Qb/sandy input intervals match to localized concentration of shells and/or to dark horizons highlighted by X-ray imaging, with the latter tentatively interpreted as the result of the compaction *P. oceanica* remains (Figs. 4 and 8). Apart from the tephra layer, no significant relationship was found between physical properties (susceptibility and γ density) and the Cluster Qb /sandy input intervals. This is likely due to a heavy

input of carbonatic/organic material (foraminifera shells and *P. oceanica* remains, respectively) from the near shore.

Due to the presence of displaced epiphytic foraminifera with abundance >25% of the total assemblage and of a relative increase in the fine sand component, we tentatively attribute the eleven intervals to episodic high energy events ($E_{1\text{-}11}$ hereinafter). These events should be related to an uncommon mechanism able to transport epiphytic species at greater depths (70 m bsl), relative to their living zone (up to 35-40 m bsl considering the depth limit of the *P. oceanica*), along with some amount of sand characterized by a peculiar grain-size distribution. The P/B ratio and X-ray imaging features can be considered only secondary evidence of the high energy events, due to their non unique correlation, with respect to those discussed above.

Apart from the 11 MS-06 high energy events, we have noticed that between ca. 2 and 2.50 m depth there is a consistent sandy input, a decrease in the P/B ratio and an epiphytic assemblage up to 23% (samples at 2.43 and 2.20 m) that did not fall in the Qb Cluster because these values resulted as <25% (see Fig. 7). However, considering the positive correlation between sedimentological and micropaleontological characteristics, we think that this layer also should be taken into consideration as a possible further high energy event that we refer to as Ex.

To obtain a good age estimate for the high-energy events, we adopted the depositional model described in the previous paragraph for the MS-06 core (Fig. 6). We started from the concept that each of the events $E_{1\text{-}11}$ represents an exceptional mass transport episode and thus, the age of the sample at the base of each interval, highlighted by the Cluster Qb, is assumed to represent the age of the event. Figure 8 reports the 2 σ age range (95% probability) for events $E_{1\text{-}11}$ and Ex, obtained on the basis of this latter assumption. Even though the depositional model helps reducing age uncertainties, the fact that we dated marine samples, requesting the use of a marine calibration curve (Reimer et al., 2009) with a ΔR offset (Reimer and Reimer, 2001), produces quite a wide interval (as long as 500 yrs) for the age of events (2σ probability range), sometimes substantially

overlapping and not allowing us to define individual separated ages (as in the case of E7 and E8, Fig. 8).

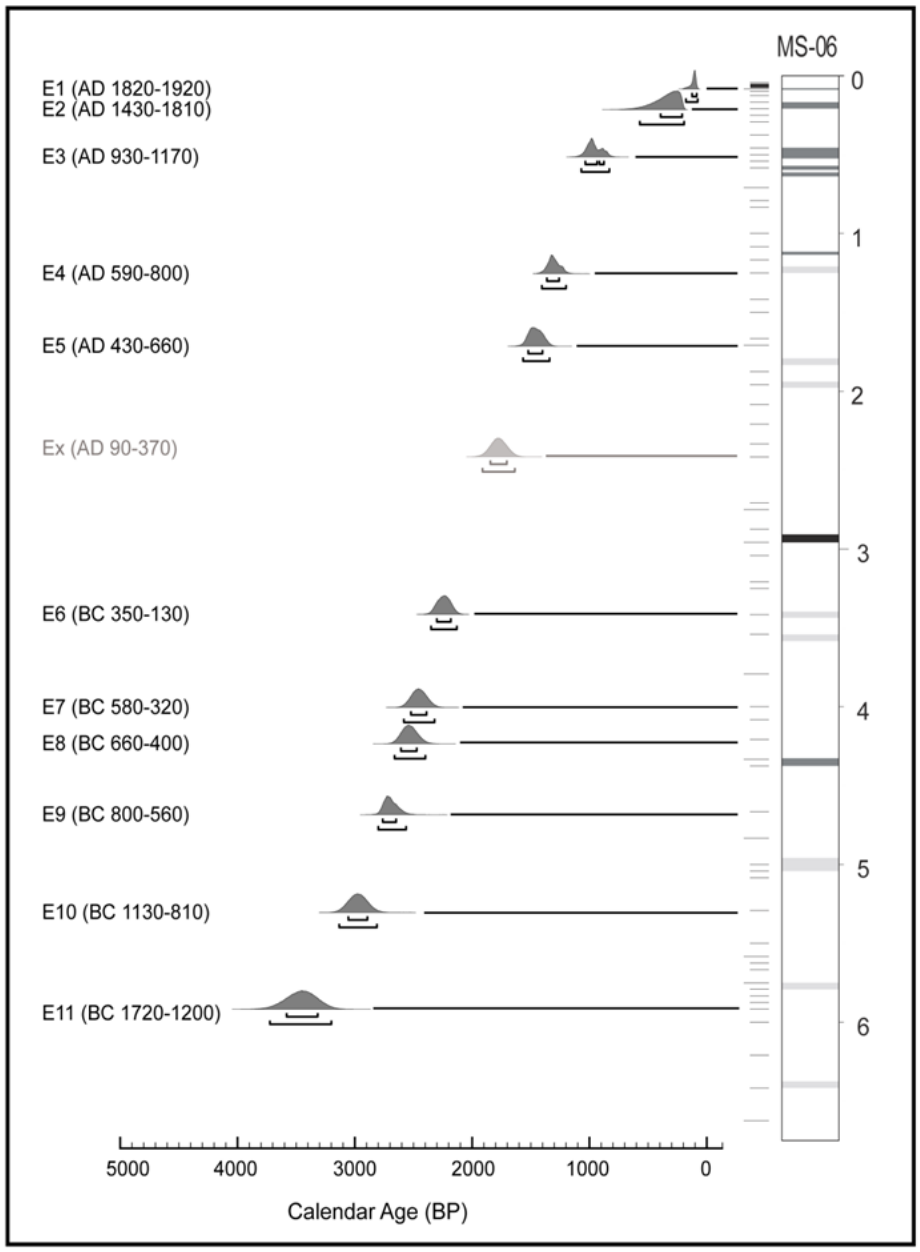

Fig. 8. Probability distribution ranges (2σ) of the modelled age of events (E1-11) obtained using P_Sequence from OxCal 4.1 software by Bronk Ramsey (2008). For legend of the core log see also Fig. 2.

5. Discussion

5.1 Triggering mechanisms and correlation with historical events

Epiphytic foraminifera living in association with seagrass meadows (e.g. *Posidonia oceanica*) have been widely studied (e.g. Langer, 1993; Wilson, 2007; Mateau-Vicens, 2010), not only for taxonomic purposes but also from an ecological standpoint. In the Mediterranean Sea, epiphytic foraminifera are very diverse and abundant so that sediments beneath seagrass and algae are rich in dead foraminifera washed from the plants. As a consequence, the latter peculiar association can be considered ecologically representative of the epiphytic assemblages and can be displaced at different water depths, generally during storms. Transport is commonly towards the shore, but occasionally patches of uprooted vegetation with their benthic assemblage can float to the open sea (Murray, 2006). This phenomenon, known as "floating plants", was observed in oceans affected by big storms (e.g. hurricanes and typhoons) or in areas susceptible to intense gravitational transport due to slope instability. However, no detailed quantitative studies currently exist regarding epiphytic foraminifera in open sea deposits.

We propose the hypothesis that the twelve MS-06 high energy events, defined on the basis of high concentration of displaced epiphytic foraminifera coupled with grain-size changes, could be related to high energy exceptional events able to disperse an extra amount of infralittoral epiphytic species toward deeper areas. These events are exceptional at the MS-06 location as we can count only 12 of them over the past 4500 yrs. Since these events are expected to be related to a remarkable washing of *P. oceanica* blades, we should also consider possible, rare, triggering mechanisms, other than storms, like earthquake shaking or tsunamis. We exclude the effects of (i) turbidity currents, because they involve base erosion and important changes in the sedimentary sequence not observed in MS-06 core and, (ii) significant environmental changes in terms of water depth or climate, as shown by micropaleontological analyses and geophysical survey.

Storms are responsible for important uprooting and transportation of *P. oceanica* blades toward the coasts and for their deposition on beaches. Because storms dissipate most of their energy by hitting the coast, they have low transportation potential toward the open sea. However, storms together with bottom currents are likely responsible for the continuous recovering of *Posidonia* fibers and for the accumulation of a small percentage of displaced epiphytic foraminifera also in open sea areas. In MS-06 the concentrations <25% of Cluster B epiphytic foraminifera can be the result of this storm action. Moreover, storms in the Mediterranean Sea are mainly related to cyclonic areas that breed in the Atlantic Ocean or in northwestern Europe. Only a few of these develop into extreme events in localized regions (e.g. southern Tyrrhenian Sea, Ionian Sea, etc.) and occur mainly during winter. From a meteorological observations data set (European Center for Medium-Range Weather Forecasts, ERA-40 Data Archive: a re-analysis of global atmosphere and surface conditions from September 1957 through August 2002 – available at: http://www.ecmwf.int/products/data/archive/descriptions/e4), we know that nine strong cyclones developed in the study area during the past 45 years. Extrapolating this average frequency on the MS-06 timeline, we would expect roughly 900 exceptional storms that could be reduced to ca. 45, if we considered the possibility of only one "exceptional storm" per century. Thus, in MS-06, we would expect an amount of high-energy events substantially larger than the number of observed ones. This makes considering the storm hypothesis unlikely. **Earthquake shaking** could be responsible for material delivering from near shore to deeper areas and could also trigger submarine slides. Because of the lack of geophysical evidence for large liquefaction structures, recent submarine slides and important mass transport deposits in the offshore area, it seems unlikely that, although local, shaking produced by earthquakes, could uproot a large amount of *P. oceanica* blades, transporting them toward the open sea. Even considering this as a possibility, we noted that the ages of the high-energy events (Fig. 8) are compatible both with local (1693, 1169) and distant earthquakes (1908, AD 365).

Thus, although earthquake shaking might be a cause for displacement of foraminifera, it is not sufficient to explain all the detected events, considering the variability of the peak ground acceleration at the study site related to the above-mentioned earthquakes.

Tsunamis are usually characterized by long wavelengths (up to some 100 km, Fujiwara, 2008) clearly greater than the ocean depth, and may involve the entire water column. This implies that a tsunami wave could affect the seabed even in open waters. Although little is known about the effects of strong tsunamis on shallow-shelf regions, such events are expected to cause important erosion from sea bottom re-suspending and transporting sand and other material more than 1 km inland (Abrantes et al., 2008 and references therein). Also the backwash effects remain speculative because there are no reliable measurements of this process. However, a video footage of the 26 December 2004 Indian Ocean tsunami, which showed great plumes of turbid water moving offshore, suggests that tsunami backwash flow velocities can be exceptionally high (Dawson and Stewart, 2007). There is little or no empirical data on backwash hydraulics, but they are clearly erosive enough to rework the onshore deposits deposited during run-up (Dawson, 1994; Nanayama et al., 2000) and may even be able to induce the corrosion and cavitation of bedrock platforms (Aalto et al., 1999; Dawson and Stewart, 2007). Their erosion undoubtedly results from the fact that coastal topography and bathymetry serve to concentrate the backwash into channelized flows (Einsele et al., 1996; Le Roux and Vargas, 2005). Moreover, from their study on living benthic foraminifera from shallow shelf sediments collected after the 2004 Indian Ocean event, Sugawara et al. (2009) suggest that accumulation of allochthonous foraminifers can be preserved as traces of paleotsunami backwash in offshore sedimentary environment. Thus, tsunami backwash waves seem to be an effective mechanism in producing both uprooting and seaward transportation of *P. oceanica* blades and their benthic biota.

Distinguishing between storm and tsunami deposits has long been a central challenge within tsunami research. Tsunami and storm waves differ in the depth to which they can disturb the sea bottom; as water depth increases, storm influence becomes less apparent, while tsunami influence

remains (Weiss and Bahlburg, 2006), and these influences could be visible in particle-size distributions (see Fig. 7). The lack of any erosion feature or sharp grain-size changes in the MS-06 record is probably due to the distance of the core site from the coast (more than 2 km) and/or to local conditions.

One further element that supports the tsunami driven mechanism is the coincidence between some of our events ages and the historical tsunamis that hit the area. It is noteworthy how the youngest three events (E1, E2 and E3) are imbedded between 1820-1920, 1430-1810 and 930-1170 AD, encompassing the dates of the major tsunamis (1908, 1693, and 1169, see Tinti et al., 2007) that are known to have hit eastern Sicily in historical times (Table 2). Furthermore, it is interesting to note that the age of the Ex event also falls into the age interval AD 90-370 that encompasses the AD 365 Crete earthquake and tsunami event. Contemporary historical reports attest that, in AD 365 "there was an earthquake throughout the world, and the sea flowed over the shore, causing suffering to countless people in Sicily and many other islands" (Jerome, 380). Based on this, we infer that the MS-06 core display the effects produced by the AD 365 tsunami on the sea bottom, as recently suggested by tsunami wave modeling efforts (Lorito et al., 2008; Shaw et al., 2008).

Table 2

Age ranges of the 12 MS-06 events correlated with historical and geological tsunami evidence from the Augusta Bay onshore.

MS-06 Events	Historical tsunamis	De Martini et al. (2010)	Scicchitano et al. (2007; 2010)	Barbano et al. (2010)	Vött et al. (2006; 2009)
E1 (AD 1820-1920)	1908 (Messina)		1908		
E2 (AD 1430-1810)	1693	PR01 (AD 1420-1690)	1693	1693	
E3 (AD 930-1170)	1169		1169	} after AD 650-930	
E4 (AD 590-800)		AU00 (AD 650-770)			AD 840
E5 (AD 430-660)					
Ex (AD 90-370)	AD 365 (Crete)	PR02 (AD 160-320)	AD 365		AD 430±40
E6 (BC 350-130)					} BC 300±60
E7 (BC 580-320)		} AU01 (BC 600-400)			
E8 (BC 660-400)					
E9 (BC 800-560)		PR03 (BC 800-600)			
E10 (BC 1130-810)		AU02 (BC 975-800)			BC 1000±200
E11 (BC 1720-1200)	BP 3600 (Santorini)	PR04 (BC 2100-1635)			

Historical tsunamis are retrieved from Tinti et al. (2007) except for the age of the Santorini event (Friedrich et al., 2006).The initials AU and PR refer respectively to the Augusta and Priolo sites investigated by De Martini et al. (2010).

5.2 Regional and supra-regional potential correlative tsunami deposits

At a regional scale, we noticed that the age of seven events identified in the offshore sediments (E2, E4, Ex, E7-8, E9, E10 and E11) show a positive correlation with the age of tsunami deposits found onshore along the Augusta Bay coastline (PR01, AU00, PR02, AU01, PR03, AU02, PR04 respectively; Table 2). Moreover, within a radius of about 25 km from the offshore coring site, onshore displaced boulders (Scicchitano et al., 2007) and coarse marine sediments (Scicchitano et al., 2010) were tentatively associated with the 1908, 1693, 1169 and 365 AD tsunami events. Further south (ca 50 km) in the Vendicari Natural Reserve area, displaced boulders have been recently interpreted as tsunami deposits and tentatively associated with two tsunamis, the 1693 and an event occurred after 650-930 AD (Barbano et al., 2010).

Thus, in terms of local (regional) tsunami hazard, the presence of 12 high energy events in the offshore (only eight in inland) testify that the marine environment can offer a continuous record definitely more sensitive to environmental change/anomalous events.

On a larger (supra-regional) scale, potential correlative deposits were identified in the Lefkada area (Greece, Ionian side) located about 500 km to the east-northeast with respect to the Augusta Bay area. In fact, intense onshore research work (Vött et al., 2006, 2009) done on washover fans, displaced boulders and marine sediments testifies the occurrence of multiple tsunami inundations in Lefkada. Specifically, the age of four tsunami events, dated at ca 840 AD, 430±40 AD, 300±60 BC and 1000±200 BC, fits perfectly with the age of the E4, Ex, E6-7, E10 events recognized in this work (Table 2).

Finally, we should mention that the age of another possible event (E11 in Table 2) could be tentatively correlated with an older tsunami that took place in the broad Eastern Mediterranean, due to the collapse of the Thera Volcano, now known as Santorini island, at ca. BP 3600 (Friedrich et al., 2006). In fact, investigations at Santorini indicate that the paroxysmal eruption (the Late Bronze Age or LBA eruption) of ca. BP 3600 was very large and may have generated multiple tsunamis. The LBA eruption had four phases, reflecting vent geometries and eruption mechanisms (Dominey-Howes, 2004 and reference therein), and tsunamigenic conditions prevailed during successive phases of the eruption. Due to the lack of contemporary historical reports, evidence of the LBA tsunami comes from geological evidence onshore (McCoy and Heiken, 2000; Minoura et al., 2000; Dominey-Howes, 2004; Bruins et al., 2008) and in the deep-sea floor of the Eastern Mediterranean (Kastens and Cita, 1981; Cita et al., 1996; Cita and Aloisi, 2000) as far as 600 km from the volcano, further testifying its supra-regional importance. If the waves originated from this event were strong enough to reach the coast of Israel, 1000 km away (Goodman-Tchernov et al., 2009), then presumably other coastal sites across the Mediterranean littoral were likely affected as well.

6. Conclusions

The multidisciplinary study of core MS-06 highlighted the occurrence, during the past 4500 yrs, of at least 12 anomalous layers, characterized mainly by the presence of displaced epiphytic benthic foraminifera and a relative increase of grain-size in the sediments. These anomalous layers could

have been caused by high-energy events, with tsunamis as best candidates. This hypothesis is also supported by the observation that the dates of four of these high energy events coincide with that of well known historical tsunamis (1908, 1693, 1169, 365 AD) and five with tsunami deposits found inland (De Martini et al., 2010). Among these latter, the oldest event also could be tentatively correlated with the Santorini tsunami event at ca. BP 3600 (Friedrich et al., 2006), and would represent the first evidence found offshore to the west. At a supra-regional scale, the MS-06 events fit well with other four tsunami evidence found onshore (Vött et al., 2006, 2009). Considering the whole set of events occurred during the past 3700 yrs, a first approximate average recurrence-time of 330-370 yrs for tsunami inundations in the Augusta Bay can be estimated.

These results suggest that our approach in the study of tsunami records is promising to define a cause-and-effect relationship between tsunamis and displaced epiphytic foraminifera rich layers. Augusta Bay represents a unique case study because it allows a comparison between geological and historical records. A comparative study between transport modeling of sediments during storms and tsunamis could also be a useful tool to better discriminate these phenomena in shallow-shelf areas. Our study could give new perspectives in the paleotsunami research and for the development of innovative approaches, which could be tested and applied in several other Mediterranean sites prone to tsunami hazard. These results are also relevant to environmental risk management and Civil Protection applications, taking into account that the Augusta Bay area is a major national industrial and military site.

Acknowledgments

This work was funded by Italian Civil Protection Department in the frame of the 2004-2006 agreement with Istituto Nazionale di Geofisica e Vulcanologia–INGV (Seismological Project S2) and by E.C. project 196 TRANSFER (contract n. 037058). We are indebted with M. Mancini for the help provided in the core logging and sampling and R. Civico for the physical properties analysis. Many thanks also to E. Lipparini and G. Marozzi for the technical support kindly offered

in the ISMAR-CNR labs. Prof. E. Gliozzi from Roma Tre University is thanked for the permission to use the micropaleontological laboratory. L. Miraglia is kindly acknowledged for assistance of SEM-EDS analyses performed at Istituto Nazionale di Geofisica e Vulcanologia, Sezione di Catania. M. Iorio (CNR-IAMC), N. Chagatay (EMCOL-ITU) and T. Goslar (Poznan University) are kindly thanks for the measurements and related discussions. We are indebted with S. Barbano (University of Catania) that helped us for the logistic of the sampling and permissions in the Augusta Bay. Thanks are due to C. Marcus for the English reviewing of the manuscript.

We wish to thank Dr. S. Kortekaas and an anonymous reviewer whose suggestions contributed to substantionally improve the original manuscript.

References

Aalto, K.R., Aatlo, R., Garrison-Laney, C.E., Ambramson, H.F., 1999. Tsunami (?) sculpturing of the pebble beach wave-cut platform, Crescent City area, California. Journal of Geology 107, 607–622.

Abrantes, F., Alt-Epping, U., Lebreiro, S., Voelker, A., Schneider, R., 2008. Sedimentological record of tsunamis on shallow-shelf areas: The case of the 1969 AD and 1755 AD tsunamis on the Portuguese Shelf off Lisbon. Marine Geology 249 (3-4), 283-293.

AGIP, 1982. Foraminiferi Padani (Terziario e Quaternario): Plate I–LII. AGIP, Milano.

Appleby, P.G., Oldfield, F., 1992. Applications of ^{210}Pb to sedimentation studies. In Ivanovich, M., and Harmon, R.S., (Eds.), Uranium-series disequilibrium. Applications to earth, marine and environmental sciences. 2nd edition. Oxford Science, Oxford, pp.731-738.

Atwater, B.F., Moore, A.L., 1992. A Tsunami About 1000 Years Ago in Puget Sound, Washington. Science 258 (5088), 1614-1617.

Barbano, M.S., Pirrotta, C., Gerardi, F., 2010. Large boulders along the south-eastern Ionian coast of Sicily: storm or tsunami deposits? Marine Geology 275, 140-154. doi:10.1016/j.margeo.2010.05.005.

Bellucci, L.G., Frignani, M., Cochran, J.K., Albertazzi, S., Zaggia, L., Cecconi, G., Hopkins, H., 2007. ^{210}Pb and ^{137}Cs as chronometers for salt marsh accretion in the Venice Lagoon-Links to flooding frequency and climate change. Journal of Environmental Radioactivity 97, 85–102.

Bronk Ramsey, C., 2008. Deposition models for chronological records. Quaternary Science Reviews 27 (1-2), 42-60.

Bronk Ramsey, C., 2009. Bayesian analysis of radiocarbon dates. Radiocarbon 51 (1), 337-360.

Bruins, H.J., MacGillivray J.A., Synolakis, C.E., Benjamini, C., Keller, J., Kisch H.J., Klügel, A., van der Plicht, J., 2008. Geoarchaeological tsunami deposits at Palaikastro (Crete) and the Late Minoan IA eruption of Santorini. Journal of Archaeological Science 35, 191-212.

Budillon, F., Ferraro, L., Hopkins, T.S., Iorio, M., Tonielli, R., Bellonia, A., D'Isanto, C., Scotto, P., 2005. Morphology and surface geology of the Augusta Bay (Eastern Ionian Sea): results of geophysical surveys. Geophysical Research Abstracts 7, 10128.

Budillon, F., Ferraro, L., Hopkins, T.S., Iorio, M., Lubritto, C., Sprovieri, M., Bellonia, A., Marzaioli, F., Tonielli, R., 2008. Effects of intense anthropic settlement of coastal areas on sea-bed and sedimentary systems: a case study from the Augusta Bay (Southern Italy). Rendiconti online della Società Geologica Italiana 3, 142-143.

Cimerman, F., Langer, M.R., 1991. Mediterranean Foraminifera. Academia Scientiarum et Artium Slovenica Classis IV 30, Ljubljana, 118 pp.

Cita, M.B., Aloisi, G., 2000. Deep-sea tsunami deposits triggered by the explosion of Santorini (3500 y BP), eastern Mediterranean. Sedimentary Geology 135, 181–302.

Cita, M.B., Camerlenghi, A., Rimoldi, B., 1996. Deep-sea tsunami deposits in the eastern Mediterranean: new evidence and depositional models. Sedimentary Geology 104, 155–173.

Cochran, U., Berryman, K., Zachariasen, J., Mildenhall, D., Hayward, B., Southall, K., Hollis, C., Barker, P., Wallace, L., Alloway, B., Wilson, K., 2006. Paleoecological insights into subduction zone earthquake occurrence, eastern North Island, New Zealand. Geological Society of America Bullettin 118, 1051-1074.

Coltelli, M., Del Carlo, P., Vezzoli, L., 1998. The discovery of a Plinian basaltic eruption of Roman age at Mt. Etna. Geology 26, 1095-1098.

Corsaro, R.A., Pompilio, M., 2004. Dynamics of magmas at Mount Etna, in: Bonaccorso, A., Calvari, S., Coltelli, M., Del Negro, C., Falsaperla, S. (Eds.), Mt. Etna: Volcano Laboratory. AGU Geophysical Monograph Series 143, pp. 91-110.

Dawson, A.G., 1994. Geomorphological processes associated with tsunami run-up and backwash. Geomorphology 10, 83–94.

Dawson, A.G., Hindson, R., Andrade, C., Freitas, C., Parish, R., Bateman, M., 1995. Tsunami sedimentation associated with the Lisbon earthquake of 1 November AD1755: Boca de Rio, Algarve, Portugal. The Holocene 5 (2), 209-215.

Dawson, A.G., Stewart, I., 2007. Tsunami deposits in the geological record. Sedimentary Geology 200 (3–4), 166–183.

Decembrini, F., Hopkins, T.S., Azzaro, F., 2004. Variability and sustenance of the deep chlorophyll maximum over a narrow shelf, Augusta Gulf (Sicily). Chemistry and Ecology 20 (1), 231-247.

Del Carlo, P., Vezzoli, L., Coltelli, M., 2004. Last 100 ka tephrostratigraphic record of Mount Etna. In: "Mt. Etna: Volcano Laboratory" Bonaccorso, A., Calvari, S., Coltelli, M., Del Negro, C., Falsaperla, S., (Eds), AGU Geophysical Monograph Series volume 143, 77-89.

De Martini, P.M., Barbano, M.S., Smedile, A., Gerardi, F., Pantosti, D., Del Carlo, P., Pirrotta, C, 2010. A 4000 yrs long record of tsunami deposits along the coast of the Augusta Bay (eastern Sicily, Italy): paleoseismological implications. Marine Geology 276, 42-57. doi:10.1016/j.margeo.2010.07.005

Di Leonardo, R., Bellanca, A., Capotondi. A., Cundy, A., Neri, R., 2007. Possible impacts of Hg and PAH contamination on benthic foraminiferal assemblages: An example from the Sicilian coast, central Mediterranenan. Science of the Total Environment 338, 168-183.

Di Leonardo, R., Bellanca, A., Neri, R., Tranchida, G., Mazzola, S., 2009. Distribution of REEs in box-core sediments offshore an industrial area in SE Sicily, Ionian Sea: Evidence of anomalous sedimentary inputs. Chemosphere 77, 778-784.

Dominey-Howes, D.T.M., 2004. A re-analysis of the Late Bronze Age eruption and tsunami of Santorini, Greece, and the implications for the volcano-tsunami hazard. Journal of Volcanology and Geothermal Research 130, 107-132.

Dunlop, J.I., 1992. Measurement of acoustic attenuation in marine sediments by impedance tube. Journal of the Acoustical Society of America, 91, 460–469.

Einsele, G., Chough, S.K., Shiki, T., 1996. Depositional events and their records — an introduction. Sedimentary Geology 104, 1–9.

Fiorini, F., Vaiani, S.C., 2001. Benthic foraminifers and transgressive–regressive cycles in the Late Quaternary subsurface sediments of the Po Plain near Ravenna (Northern Italy). Bollettino della Società Paleontologica Italiana 40, 357–403.

Friedrich, W.L., Kromer, B., Friedrich, M., Heinemeier, J., Pfeiffer, T., Talamo, S., 2006. Santorini eruption radiocarbon dated to 1627-1600 B.C. Science 312, 548.

Fujiwara, O., 2008. Bedforms and sedimentary structures characterizing tsunami deposits. In: Shiki, T., Tsuji, Y., Yamazaki, T., Minoura, K., (Eds.), Tsunamiites - Features and Implications, pp. 51-62. Elsevier, Amsterdam.

Gasperini, L., 2005. Extremely shallow-water morphobathymetric surveys: The Valle Fattibello (Comacchio, Italy) test case. Marine Geophysical Researches 26, 97–107. doi:10.1007/s11001-005-3710-0

GAZZETTA UFFICIALE DELLA REPUBBLICA ITALIANA (G.U.R.I.). Decreto Ministeriale 6 novembre 2003, no 367. Regolamento concernente la fissazione di standard di qualità

nell'ambiente acquatico per le sostanze pericolose, ai sensi dell'articolo 3, comma 4, del decreto legislativo 11 maggio 1999, n. 152, vol. 5. Ministero dell'Ambiente e della Tutela del Territorio, Roma, 08 Gennaio; 2004. pp. 17–29.

Goodman-Tchernov, B.N., Dey, H.W., Reinhardt E.G., McCoy F., Mart Y., 2009. Tsunami waves generated by the Santorini eruption reached Eastern Mediterranean shores. Geology 37, 943-946.

Hammer, Ø., Harper, D., 2006. Paleontological Data Analysis. Blackwell Publishing, Oxford.

Hammer, Ø., Harper, D.A.T., Ryan, P.D., 2001. PAST: Paleontological Statistics Software Package for Education and Data Analysis. Palaeontologia Electronica 4 (1), 9 pp. http://palaeo-electronica.org/2001_1/past/issue1_01.htm

Horn, H.S., 1966. Measurement of "overlap" in comparative ecological studies. American Naturalist 100, 419–424.

Jarosewich, E., Nelen, J.A., Norberg, J.A., 1980. Reference samples for electron microprobe analysis. Geostandards Newsletter 4 (1), 43-47.

Jerome, 380. Chronicon Eusebii, Eusebius Chronicon, ed R. Helm, GSC 47, Berlin 1956.

Jorissen, F.J., 1987. The distribution of benthic Foraminifera in the Adriatic Sea. Marine Micropaleontology 12, 21-48.

Kastens, K.A., Cita, M.B., 1981. Tsunami-induced transport in the abyssal Mediterranean Sea. Geological Society of America Bulletin 92, 845-857.

Langer, M., 1993. Epiphytic Foraminifera. Marine Micropaleontology 20, 235-265.

Le Bas, M.J., Le Maitre, R.W., Streckeisen, A., Zanettin, B.A., 1986. Chemical classification of volcanic rocks based on the total alkali-silica diagram. Journal of Petrology 27, 745-750.

Le Roux, J.P., Vargas, G., 2005. Hydraulic behavior of tsunami backflows: insights from their modern and ancient deposits. Environmental Geology 49, 65-75.

Lorito, S., Tiberti, M.M., Basili, R., Piatanesi, A., Valensise, G., 2008. Earthquake-generated tsunamis in the Mediterranean Sea: Scenarios of potential threats to Southern Italy. Journal Geophysical Research 113, B01301, doi:10.1029/2007JB004943.

Martuzzi, M., Mitis, F., Buggeri, A., Terracini, B., Bertollini, R., Gruppo Ambiente e Salute Italia, 2002. Ambiente e stato di salute nella popolazione delle aree ad alto rischio di crisi ambientale in Italia. Epidemiologia & Prevenzione 26, 1–53.

Mateu-Vicens, G., Box, A., Deudero, S., Rodríguez, B., 2010. Comparative analysis of epiphytic foraminifera in sediments colonized by seagrass *Posidonia oceanica* and invasive macroalgae *Caulerpa* spp. Journal of Foraminiferal Research 40 (2), 134-147.

McCoy, F., Heiken, G., 2000. Tsunami generated by the Late Bronze Age eruption of Thera (Santorini), Greece. Pure and Applied Geophysics 157, 1227–1256, doi:10.1007/s000240050024

Minoura, K., Imamura, F., Kuran, U., Nakamura, T., Papadopoulos, G.A., Takahashi, T., Yalciner, A.C., 2000. Discovery of Minoan tsunami deposits. Geology 28, 59-62.

Morisita, M., 1959. Measuring of interspecific association and similarity between communities. Memoirs of the Faculty of Science 3, Kyushu University, pp. 65–80.

Murray, J.W., 2006. Ecology and applications of Benthic Foraminifera. Cambridge University Press, Cambridge.

Nanayama, F., Shigeno, K., Satake, K., Shimokawa, K., Koitabashi, S., Miyasaka, S., Ishii, M., 2000. Sedimentary differences between the 1993 Hokkaido-Nansei-Oki tsunami and the 1959 Miyakojima typhoon at Taisea, southwestern Hokkaido, northern Japan. Sedimentary Geology 135, 255–264.

Pantosti, D., Barbano, M.S., Smedile, A., De Martini, P.M., Tigano, G., 2008. Geological Evidence of Paleotsunamis at Torre degli Inglesi (northeast Sicily). Geophysical Research Letters 35, L05311doi:10.1029/2007GL032935.

Parker, W.C., Arnold, A.J., 1999. Quantitative analysis in foraminiferal ecology. In: Sen Gupta, B. (Ed.), Modern Foraminifera. Kluver Academic Publisher, New York, pp. 71-79.

Perés, J.M., and Picard, J., 1964. Nouveau manuel de Bionomie bentique de la mer Mediterranée. Rec. Trav. Station Marine d'Endoume 31 (47), 1-137.

Pergent, G., Pergent-Martini, C., Boudouresque, C.F., 1995. Utilisation de l'herbier a *Posidonia oceanica* comme indicateur biologique de la qualiteé du milieu littoral en Méditerranée: état des connaissances. Mesogée 54, 3–27.

Pinegina, T.K., Bourgeois, J., Bazanova, L.I., Melekestsev, I.V., Braitseva, O.A., 2003. A millennial-scale record of Holocene tsunamis on the Kronotskiy Bay coast, Kamchatka, Russia. Quaternary Research 59, 36-47.

Raffa, F., Hopkins. T.S., 2004. Circulation and water mass structure over a narrow shelf, Augusta Gulf (Sicily). Chemistry and Ecology 20 (1), 249-266.

Reimer, P.J., Baillie, M.G.L., Bard, E., Bayliss, A., Beck, J.W., Blackwell, P.G., Bronk Ramsey, C., Buck, C.E., Burr, G.S., Edwards, R.L., Friedrich, M., Grootes, P.M., Guilderson, T.P., Hajdas, I., Heaton, T.J., Hogg, A.G., Hughen, K.A., Kaiser, K.F., Kromer, B., McCormac, F.G., Manning, S.W., Reimer, R.W., Richards, D.A., Southon, J.R., Talamo, S., Turney, C. S.M., van der Plicht, J., Weyhenmeyer, C.E., 2009. IntCal09 and Marine09 radiocarbon age calibration curves, 0-50,000 years cal BP. Radiocarbon 51 (4), 1111-1150.

Reimer, P.J., McCormac, F.G., 2002. Marine radiocarbon reservoir corrections for the Mediterranean and Aegean Seas. Radiocarbon 44, 159-166.

Reimer, P.J., Reimer, R.W., 2001. A marine reservoir correction database and on-line interface. Radiocarbon 43, 461-463. [suppl. mat.URL:http://www.calib.org)].

Reinhardt, E.G., Goodman, B.N., Boyce, J.I., Lopez, G., van Hengstum, P., Rink, W.J., Mart, Y., Raban, A., 2006. The tsunami of 13 December A.D. 115 and the destruction of Herod the Great's harbor at Caesarea Maritima, Israel. Geology 34, 1061–1064.

Robbins, J.A., 1978. Geochemical and geophysical application of radioactive lead. In: Nriagu J.O. (Ed.) The biogeochemistry of lead in the environment. Elsevier, Amsterdam

Scheffers, A., Kelletat, D., Vött, A., May, S.M., Scheffers, S., 2008. Late Holocene tsunami traces on the western and southern coastlines of the Peloponnesus (Greece). Earth and Planetary Science Letters 269, 271–279.

Scicchitano, G., Costa, B., Di Stefano, A., Longhitano, S., Monaco, C., 2010. Tsunami and storm deposits preserved within a ria-type rocky coastal setting (Siracusa, SE Sicily). Zeitschrift für Geomorphologie N.F. 54 (3), 51-77.

Scicchitano, G., Monaco, C., Tortorici, L., 2007. Large boulder deposits by tsunami waves along the Ionian coast of south-eastern Sicily (Italy). Marine Geology 238, 75–91.

Sgarrella, F., Moncharmont Zei, M., 1993. Benthic foraminifera of the Gulf of Naples (Italy): systematics and autoecology. Bollettino della Società Paleontologica Italiana 32, 145–264.

Shaw, B., Ambraseys, N.N., England, P.C., Floyd, M.A., Gorman, G.J., Higham, T.F.G., Jackson, J.A., Nocquet, J.M., Pain, C.C., Piggott M.D., 2008. Eastern Mediterranean tectonics and tsunami hazard inferred from the AD 365 earthquake. Nature Geoscience 1, 268-276, doi: 10.1038/ngeo151 Article

Shiki, T., Tachibana, T., Fujiwara, O., Goto, K., Nanayama, F., Yamazaki, T., 2008. Characteristic features of tsunamiites. In: Shiki, T., Tsuji, Y., Yamazaki, T., Minoura, K., (Eds.), Tsunamiites - Features and Implications, Elsevier, Amsterdam, pp. 319-340.

Shumway, G., 1960. Sound speed and absorption studies of marine sediments by a resonance method. Geophysics 25, 451-467.

Sugawara, D., Minoura, K., Nemoto, N., Tsukawari, S., Goto, K., Imamura, F., 2009. Foraminiferal evidence of submarine sediment transport and deposition by backwash during 2004 Indian Ocean tsunami. Island Arc 18, 513-525.

Tinti, S., Maramai, A., Graziani, L., 2007. The Italian Tsunami Catalogue (ITC), Version 2. Available on-line at: http://www.ingv.it/servizi-e-risorse/BD/catalogo-tsunami/catalogo-degli-tsunami-italiani

Van der Bergh, G.D., Boer, W., Haas, H., van Weering, T., van Wijhe, R., 2003. Shallow marine tsunami deposits in Telik Banten (NW Java, Indonesia), generated by the 1883 Krakatau eruption. Marine Geology 197, 13–34.

Van der Zwaan, G.J., Jorissen, F.J., 1991. Biofacial patterns in river-induced shelf anoxia. In: Tyson, R.V., Pearson, T.H., (Eds.), Modern and Ancient Continental Shelf Anoxia. Geological Society Special Publication, London, 58, pp. 65–82.

Van der Zwaan, G.J., Jorissen, F.J., de Stigter, H.C, 1990. The depth dependency of planktonic/benthic foraminiferal ratios: constraints and applications. Marine Geology 95, 1–16.

Vött, A., May, M., Brückner, H., Brockmüller, S., 2006. Sedimentary Evidence of Late Holocene Tsunami Events near Lefkada Island (NW Greece). Zeitschrift für Geomorphologie N.F. 146, 139-172.

Vött, A., Brückner, H., Brockmüller, S., Handl, M.. May, S.M., Gaki-Papanastassiou, K., Herd, R., Lang, F., Maroukian H., Nelle, O., Papanastassiou, D., 2009. Traces of Holocene tsunamis across the Sound of Lefkada, NW Greece. Global and Planetary Change 66 (1-2), 112-128.

Weiss, R., Bahlburg, H., 2006. A note on the preservation of offshore tsunami deposits. Journal of Sedimentary Research 76, 1267–1273.

Wilson, B., 2007. Guilds among epiphytal foraminifera on fibrous substrates, Nevis, West Indies. Marine Micropaleontology 63, 1–18.